Journal of Physics B: Atomic, Molecular and Optical Physics

Generating strong anti-bunching by interfering nonclassical and classical states of light

OPEN ACCESS
IOP Publishing
Journal of Physics B: Atomic, Molecular and Optical Physics
J. Phys. B: At. Mol. Opt. Phys. **52** (2019) 215401 (8pp)
https://doi.org/10.1088/1361-6455/ab3e98

Generating strong anti-bunching by interfering nonclassical and classical states of light

Rajiv Boddeda[1], **Quentin Glorieux, Alberto Bramati and Simon Pigeon**

Laboratoire Kastler Brossel, Sorbonne Université, CNRS, ENS-PSL Research University, Collège de France, 4 place Jussieu, 75252 Paris, France

E-mail: rajiv.boddeda@polytechnique.edu

Received 19 July 2019
Accepted for publication 27 August 2019
Published 8 October 2019

Abstract

In quantum optics, the second-order correlation function $g^{(2)}(\tau)$ characterizes the photon statistics of a state of light and can be used to distinguish between its classical or quantum nature. In this article, we study a simple setup which offers the possibility to generate quantum states of light with very small $g^{(2)}(0)$, a signature of strong anti-bunched light. This can be achieved by mixing on a beamsplitter a coherent state with a nonclassical state, such as a squeezed state, and even with a bunched state ($g^{(2)}(0) > 1$) such as a Schrödinger cat state. We elucidate the interference mechanism generating such strong anti-bunching and relate it to the unconventional photon blockade. We also detail how this effect can be applied to detect weakly squeezed states of light.

Keywords: quantum optics, anti-bunching, photon blockade, squeezing detection

(Some figures may appear in colour only in the online journal)

Nonclassical photon sources play a crucial role in emerging quantum technologies. Given the robustness of quantum states of light, photons are the best candidates for applications in the field of quantum communication and quantum cryptography [1, 2]. One common way of characterizing the nonclassical nature of light sources is by measuring the second-order correlation function of the field intensity, $g^{(2)}(\tau)$. The value of this function at $\tau = 0$ for classical light is larger than 1 and is equal to 1 for a coherent state. Therefore, $g^{(2)}(0) < 1$ is seen as a signature of the nonclassical nature of light [3]. It reveals that the temporal statistics of photons is sub-Poissonian (more ordered in time than a coherent source), often referred to as anti-bunched light. Anti-bunched states of light also have applications beyond quantum technologies in fields such as super-resolution microscopy. It is possible to go beyond the diffraction limit by taking advantage of ordered photon emission of strongly anti-bunched sources [4, 5].

Such states of light are typically obtained using nanoemitters such as semiconductor quantum dots [6, 7], nitrogen vacancy centers in diamonds [8], and many other solid-state sources. These sources are considered to be the most efficient single-photon sources [9]. The anti-bunching of the light emitted by these devices derives directly from the extreme confinement of matter excitations. Another way to produce anti-bunched states of light is to directly modify a coherent light beam using a non-linear medium in a cavity. A strong non-linear medium is usually required to allow only one photon at a time through the medium, a phenomena referred to as photon blockade [10, 11]. However, it has been recently proposed that anti-bunching can also be achieved by combining weak photon–photon interactions and optical path interference [12–14]. This configuration, known as unconventional photon blockade, has been realized experimentally and validated in a quantum dot system [15] and a superconducting circuit [16], paving the way for efficient sources of anti-bunched light.

In this manuscript, we focus on a quantum interference effect which allows for unconventional photon blockade, and we show how it can be exploited to create anti-bunching. We

[1] Author to whom any correspondence should be addressed.

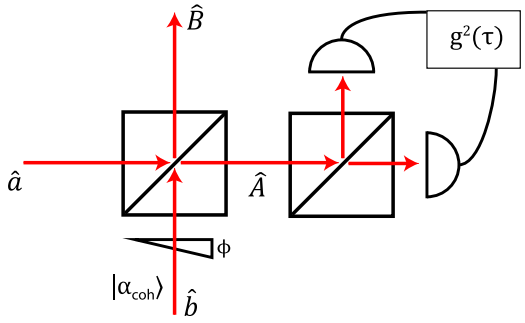

Figure 1. Schematic setup for the creation of anti-bunched states. The two input operators are indicated by $\hat{a}$ and $\hat{b}$, and the corresponding output operators are denoted by $\hat{A}$ and $\hat{B}$. The input mode $\hat{b}$ consists of a coherent state with a tunable phase ϕ relative to $\hat{a}$. Several input states $\hat{A}$ are studied in this paper. The correlation function is computed on the output mode $\hat{A}$ in the same way as is done experimentally, i.e. using a beamsplitter and two photodetectors as represented.

show that mixing even weak bunched states of light ($g^{(2)} > 1$) with coherent states of light ($g^{(2)} = 1$), can lead to strong anti-bunched states of light ($g^{(2)} \simeq 0$). This observation, initially pointed out four decades ago [3, 17], is analyzed in this paper to elucidate how interference at the level of Fock state components of the states leads to such strong anti-bunching.

The implementation of the setup only requires a beamsplitter to mix both coherent and weak nonclassical states. A single-sided cavity filled with a non-linear medium can also be used, causing the reflected part of a coherent field to interfere with the one escaping from the cavity (weak nonclassical field). However, it can be shown using the approach detailed in [18] that such a non-linear medium in a cavity can lead to $g^{(2)}(0)$ below 1, but requires a strict control on the parameters of a complex experiment.

The setup we consider here is illustrated in figure 1 and is based on two input beams labeled $\hat{a}$ and $\hat{b}$ mixed on a beamsplitter. The relative phase between both inputs ϕ can be tuned via a delay line and the beamsplitter, of reflectance R, is considered lossless. This setup is similar to the one studied in [17]. The two outputs of the beamsplitter, respectively labeled $\hat{A}$ and $\hat{B}$, can be written as

$$\begin{aligned} \hat{A} &= \sqrt{1-R}\,\hat{a} + \sqrt{R}\,\hat{b}e^{i\phi\pi}, \\ \hat{B} &= -\sqrt{R}\,\hat{a} + \sqrt{1-R}\,\hat{b}e^{i\phi\pi}, \end{aligned} \tag{1}$$

where $\phi \in [0, 2]$ (note that ϕ is normalized to π). In what follows, one of the two input states, namely $\hat{b}$, will always be a coherent state.

We focus on the statistics of one of the two outputs using a standard coincidence measurement scheme [19] corresponding to the second beamsplitter on the right in figure 1. More complex methods can also be used to quantify more accurately second- or higher-order correlations, but it comes at the cost of increased complexity of the setup [20, 21].

The statistics of a stationary field in a given electromagnetic mode can be quantified using the second-order correlation function [22]

$$g^{(2)}(\tau) = \frac{\langle \hat{A}^\dagger(0)\hat{A}^\dagger(\tau)\hat{A}(\tau)\hat{A}(0)\rangle}{\langle \hat{A}^\dagger(0)\hat{A}(0)\rangle^2}, \tag{2}$$

where $\hat{A}$ is the annihilation operator in the mode in which we would like to measure $g^{(2)}(\tau)$.

For a pure quantum state which can be expressed in the Fock state basis using $|\psi\rangle = c_0|0\rangle + c_1|1\rangle + c_2|2\rangle + c_3|3\rangle...$ [23], where the coefficients c_i can be time-dependent, the second-order correlation function corresponds to

$$g^{(2)}(\tau) = \frac{\sum_{n=2}^{\infty} n(n-1)|c_n(\tau)|^2}{\left(\sum_{n=1}^{\infty} n|c_n(0)|^2\right)^2}. \tag{3}$$

Notice that the numerator summation starts at $n = 2$, whereas the denominator starts from $n = 1$. Sub-Poissonian statistics imply that the numerator of equation (3) is smaller than its denominator. For a weak-amplitude state where $|c_n|^2$ vanishes quickly with n, anti-bunching can be achieved either by increasing $|c_1|^2$ or minimizing $|c_2|^2$. Both the single- and two-photon components are in general strongly related. The aim is to specifically cancel $|c_2|^2$ using the interference effect. In what follows, if any truncation is applied to equation (3), the convergence with respect to the truncation is always verified.

We evaluate the second-order correlation function of an output field of a beamsplitter for known input fields. By adjusting the relative phase and the reflectance of the beamsplitter, we will show how strong anti-bunching can be reached even with a weak nonclassical states. In section 1, we will focus on phase-modified coherent states to illustrate the interference effect at play between the photon number components of the input states leading to strong anti-bunching. In section 2, we will consider states that only include even photon number components. In these two first sections, we will consider two types of input states: a simplistic example to analyze the underlying physics, and a practical example to demonstrate the experimental feasibility of our setup. Finally, in the last section, we will discuss how the present proposal compares with the unconventional photon blockade (section 3).

1. Phase-modified coherent states

In this section, we consider a phase-modified coherent state, i.e. a normal coherent state to which we apply different dephasing to different Fock number states, in the Fock state basis. By considering such an input state in mode $\hat{a}$ plus a coherent state in mode $\hat{b}$, we observe clear and strong anti-bunching in $\hat{A}$ for certain optimal parameters.

Let's consider, for pedagogical purposes, a coherent state with the two-photon Fock component dephased with respect to the other Fock components and interfering with a coherent state. This state can then be written in the form

$$|\psi\rangle = \sum_{n\geqslant 0} \frac{\alpha^n}{\sqrt{n!}} e^{-\frac{|\alpha|^2}{2}} e^{i\frac{\pi}{2}\delta_{n,2}}|n\rangle, \tag{4}$$

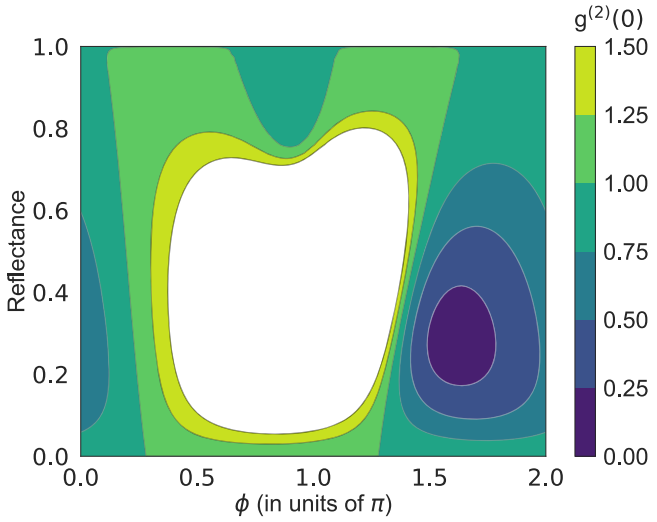

Figure 2. The correlation function of the output state, as a function of the reflectance and ϕ, for a given amplitude $\alpha = 0.3$ of the coherent state and the phase-modified state defined in equation (4). One can observe how the correlation function goes below 0.5 for low reflectance and around $\phi = 1.6$. The white region in the plot corresponds to $g^{(2)}(0) > 1.5$.

where $\delta_{n,2}$ is the Kronecker delta function and α is the amplitude of the state.

In figure 2, the $g^{(2)}(0)$ function is plotted as a function of the relative dephasing ϕ and the reflectance R. One can observe that mixing this phase-modified state, as defined in equation (4), with a coherent state allows us to generate perfect anti-bunched states in the output mode $\hat{A}$. For example, a pure anti-bunched state can be generated by considering a beamsplitter with ≈22.5% reflectance and a relative phase ϕ of approximately 1.6π, for a state amplitude of 0.3. However, we found that the minimum of the correlation function increases exponentially as a function of the number of photons in the input coherent state, $|\alpha|^2$. This example clearly shows the strong dependence of the output correlation function on the relative phase difference between the different Fock components of the incoming state.

States defined in equation (4) are nonphysical. In the following, we consider another type of state that can be realized experimentally, such as the one obtained after letting a coherent state propagate through a purely real $\chi^{(3)}$ non-linear medium. This state can be written in the following form [24]:

$$|\alpha(t)\rangle = \exp\left(-\frac{|\alpha^2|}{2}\right)\sum_n \exp\left(-i\hat{H}_{nl}t\right)\frac{\alpha^n}{\sqrt{n!}}|n\rangle$$
$$= \exp\left(-\frac{|\alpha^2|}{2}\right)\sum_n \exp\left(-i\chi^{(3)}t(n^2 - n)\right)\frac{\alpha^n}{\sqrt{n!}}|n\rangle, \quad (5)$$

with $\hat{H}_{nl}$ being the non-linear Hamiltonian and $\chi^{(3)}$ being the third-order non-linear susceptibility of the medium.

One can observe that in this case, the non-linearity implies that the phase of each Fock component evolves at a different rate, accumulating a different phase while propagating. Interfering such a state with a coherent state on a beamsplitter with an adequate relative phase between both beams and a proper reflection coefficient leads to strong anti-bunching, as shown in figure 3.

We show in the panel (a) of figure 3 the numerical evaluation of the corresponding second-order correlation of the output field $\hat{A}$ as a function of the relative phase ϕ between the two input beams and the beamsplitter reflectance R. Even though the anti-bunched region is smaller than in the previous example, we can clearly observe two dips in the correlation function map.

Here, for simplicity, we consider both input states with the same amplitude $\alpha = 0.3$. We took $\chi^{(3)}t = 0.05$ for the non-linearity required to produce the non-coherent state, which corresponds to a relatively small non-linearity easily achievable experimentally [25]. One could observe the same effect in the other output mode ($\hat{B}$) for a symmetric set of parameters ($R' = 1 - R$ and $\phi' = 1 - \phi$). An important thing to note is that the observed strong anti-bunching corresponds to a non-vanishing output intensity.

Indeed, the prospect of finding the smallest $g^{(2)}(0)$ is only relevant if the output state is not vacuum.

In the present case, we find that $g^{(2)}(0) = 0.03$ while $\langle\hat{n}\rangle \approx 0.006$ for $\alpha = 0.3$. To that purpose, we show in the panel (b) of figure 3 how the second-order correlation function and the photon number in the output arm vary with the amplitude α at the optimal condition. Here, we assume that both input states have the same amplitude. We clearly see that $g^{(2)}$ increases when increasing the input field amplitude α, and that it increases faster than the mean number of photons of the output field $\langle\hat{n}_A\rangle$. However, until $\alpha = 0.5$, we have strong anti-bunching ($g^{(2)} < 0.5$), and for $\alpha < 0.2$ the output state exhibits very strong anti-bunching ($g^{(2)} < 0.01$) with non-zero output amplitude (up to $\langle\hat{n}_A\rangle \approx 0.003$) (inset of the panel (b) of figure 3).

The setup described can be realized experimentally using a Mach–Zehnder interferometer with a non-linear medium in one of the arms. The phase ϕ is modified by tuning one arm of the interferometer.

Other nonclassical states can also be employed using the same scheme. In the following, we will focus on states only composed of even Fock components.

2. Even Fock states

In the preceding section, we have shown that when we modify the relative phase between the Fock components of a coherent state, one can produce strongly anti-bunched states. In this section, an alternative route is explored to demonstrate that this phenomenon can also be observed when the amplitudes of the Fock components are modified. We consider examples in which the odd photon components are reduced compared to the coherent states, similar to the case of even Schrödinger cat states. In these cases, mixing even a slightly nonclassical state with a coherent state will lead to the observation of strongly anti-bunched statistics. Despite the difference in the approach proposed here with respect to the previous cases, the underlying idea is identical: interfering

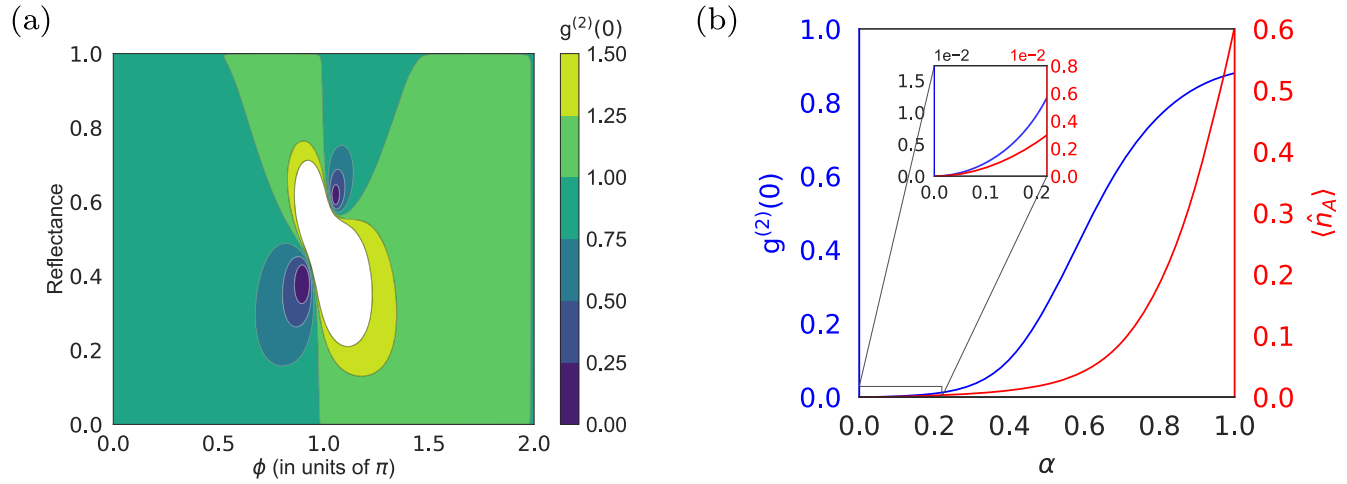

Figure 3. The correlation function, $g^{(2)}(0)$, and photon number, $\langle \hat{n}_A \rangle$, as a function of the reflectance and phase angle ϕ when considering one coherent state modified by a non-linear medium, as given in equation (5) in the input mode $\hat{a}$, and another coherent state with same amplitude $\alpha = 0.3$ in the input mode $\hat{b}$. We assume that the modified coherent state $|\alpha\rangle$ has propagated through a weak non-linear medium with the parameter $\chi t = 0.05$. (a) Correlation function at zero delay for $\hat{A}$. (b) The minimum of the $g^{(2)}(0)$ and the corresponding average photon number in mode $\hat{A}$ as a function of the coherent state amplitude in the input mode for optimal ϕ and R. Inset in (b): magnification of small α and strong anti-bunching limit.

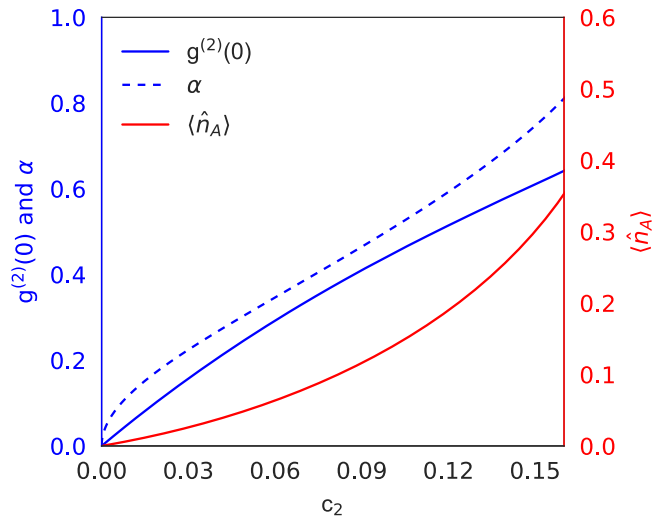

Figure 4. The second-order correlation function and the photon number at the output arm, as a function of the amplitude of the two-photon coefficient of the superposition state, c_2. The dashed blue curve corresponds to the amplitude of the coherent state to obtain the minima of $g^{(2)}(0)$ at the output arm of a 50:50 beamsplitter, the solid blue curve corresponds to $g^{(2)}(0)$, and the red curve represents the average photon number in that arm.

the two-photon Fock component of the squeezed states with that of the coherent state can generate strong anti-bunching.

2.1. Superposition of vacuum and two-photon state

We begin with a simple example: a normalized weak two-photon pure state in superposition with the vacuum defined by $|\psi\rangle = c_0|0\rangle + c_2|2\rangle$. In this case, we have $g^{(2)}(0) = 1/(2|c_2|^2) \geqslant 0.5$. If we consider this state in one of the input modes of the beamsplitter ($\hat{a}$) and a coherent state in the other input mode, i.e. both the input states with $g^{(2)}(0) \geqslant 0.5$, then the output state in the mode $\hat{A}$ can exhibit strong sub-Poissonian statistics such as $g^{(2)}(0) \ll 0.5$. In figure 4, we show how the correlation function (solid blue line) changes as a function of the amplitude of the two-photon state component c_2 of the mode $\hat{a}$ for a 50:50 beamsplitter. The $g^{(2)}(0)$ is minimized for each value of c_2 by tuning α, the amplitude of the input coherent state in the mode $\hat{b}$. The corresponding α is represented in figure 4 in the dashed blue line. The red line represents the mean photon number in the output mode $\hat{A}$. One can clearly observe that $g^{(2)}(0) \leqslant 0.5$ for $c_2 \leqslant 0.1$, even though the input state $\hat{a}$ has $g^{(2)}(0) > 50$ for $c_2 < 0.1$.

This counterintuitive example shows that mixing on a beamsplitter a state with only vacuum component and a two-photon component with a coherent state may lead to strong sub-Poissonian statistics, which is a signature of single-photon states.

2.2. Schrödinger cat states

This formalism can be extended to Schrödinger cat states. These are formed by the superposition of two coherent states with opposite phases. Depending on whether the coherent states are added or subtracted, the resulting state is either referred to as even or odd cat state, respectively. In the weak-amplitude case, if one evaluates the correlation function of odd cat states using equation (2), one can find that they exhibit anti-bunching since they only contain odd Fock states. Using such states in the present scheme and mixing them with a coherent state will always lead to an increase of $g^{(2)}(0)$ in the output arm. As the odd cat state does not encompass a two-photon component, mixing it with a coherent state will always lead to an output state with residual two-photon components, and hence a higher $g^{(2))}(0)$ in the output than in the input. To reduce $g^{(2))}(0)$, more complex schemes can be implemented to keep the c_2 at the output close to zero and

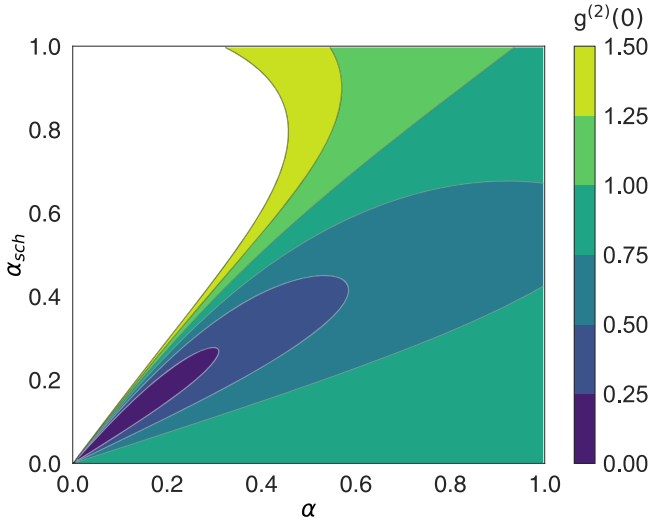

Figure 5. Contour plot of the second-order correlation function at the output arm as a function of the amplitude of the coherent state (α_b) and the amplitude of the even Schrödinger cat state ($\alpha_{\rm sch}$) in the two input arms. We consider a 50:50 beamsplitter.

reduce the three-photon component at the same time. However, this is different with the even cat states. The even cat states can be written as

$$|\text{cat}_e\rangle \propto |0\rangle + \frac{\alpha_{\rm sch}^2}{\sqrt{2}}|2\rangle + \frac{\alpha_{\rm sch}^4}{2}|4\rangle + ..., \tag{6}$$

where $\alpha_{\rm sch}$ is the cat state amplitude. Since the expressions are not tractable analytically, we evaluate the output correlations numerically using the QuTiP toolbox [26].

We assume the beamsplitter to be symmetric, i.e. 50:50. Figure 5 shows that $g^{(2)}(0)$ varies as a function of α, the amplitude of the coherent state in mode $\hat{b}$, and of α_{sch}, the amplitude of the input cat state in mode $\hat{a}$. We observe that bunching occurs if $\alpha_{sch} < \alpha$, whereas $\alpha_{sch} > \alpha$ leads to anti-bunching.

Moreover, for $\alpha_{\rm sch} \approx \sqrt{\alpha}/2$, we obtain the minimum of $g^{(2)}(0)$ where $g^{(2)}(0) \to 0$ with $\alpha \to 0$. Interestingly, the sensitivity of the autocorrelation function (local derivative with respect to α_{sch} and α) increases, while $g^{(2)}(0)$ decreases for decreasing amplitudes, which can be advantageously used to characterized even cat states.

There are several experimental techniques that can be employed to generate Schrödinger cat states [27–30]. However, characterizing such states is a very challenging task as it usually relies on full-state tomography with high sensitivity. Our simple scheme can offer an interesting alternative: a cat state of a given amplitude mixed with a coherent state can be detected by measuring the correlation function $g^{(2)}(0)$ of the output field. In addition, the variation of this value with respect to the amplitude of the input coherent field is also directly linked to the amplitude of the cat state. Both quantities, easily accessible, can be advantageously used to witness low-amplitude Schrödinger cat states.

It is known that at low amplitudes of $\alpha_{\rm sch}$, cat states converge to squeezed states which we now consider explicitly.

2.3. Squeezed coherent states

Squeezed states have been observed in many different types of systems such as parametric down conversion [31], optical fibers [32], semiconductor lasers [33], and four-wave-mixing in atomic vapor [34–36], etc. In this subsection, we see how one can use squeezed coherent states to create anti-bunching. If one considers a vacuum squeezed state, it consists of only even Fock states [37]. Hence, squeezed coherent states should be similar to the case discussed previously.

For a squeezed coherent state and a coherent state respectively in the input modes $\hat{a}$ and $\hat{b}$, the total input state can be written as

$$|\psi\rangle_{\rm input} = D(\alpha_a, \hat{a})S(\xi_a, \hat{a})|0\rangle_a \otimes D(\alpha_b, \hat{b})|0\rangle_b, \tag{7}$$

where $\hat{a}$ and $\hat{b}$ are the annihilation operators acting on the two input modes. The displacement and the squeezing parameters in the corresponding modes are denoted by $\alpha = |\alpha|e^{i\Phi}$ and $\xi = re^{i\omega}$, with superscripts indicating the modes in which they act on. In the latter, ω denotes the squeezing angle. The squeezing operator is given by $S(\xi, \hat{a}) = e^{\frac{1}{2}(\xi^*\hat{a}^2 - \xi\hat{a}^{\dagger 2})}$ and the displacement operator by $D(\alpha, \hat{b}) = e^{(\alpha\hat{b}^\dagger - \alpha^*\hat{b})}$ [23, 38].

Using the beamsplitter relations in equation (1), we can write the output state of the beamsplitter as

$$\begin{aligned}|\psi\rangle_{\rm out} = D(\alpha_a, \sqrt{T}\hat{A} - \sqrt{R}\hat{B})D(\alpha_b, e^{-i\phi}(\sqrt{R}\hat{A} + \sqrt{T}\hat{B}))\\ S(\xi_a, \sqrt{T}\hat{A} - \sqrt{R}\hat{B})(|0\rangle_A \otimes |0\rangle_B),\end{aligned} \tag{8}$$

with $T = 1 - R$ as the beamsplitter transmittance. Since the displacement operators always commute with each other, one can simplify the displacement part of the equation to $D(\alpha_b', \sqrt{R'}\hat{A} + \sqrt{T'}\hat{B})$, in which

$$\sqrt{R'} = \frac{\alpha_a}{\alpha_b'}\sqrt{T} + \sqrt{R}, \tag{9}$$

$$\sqrt{T'} = \sqrt{T} - \frac{\alpha_a}{\alpha_b'}\sqrt{R}, \tag{10}$$

$$\alpha_b' = \alpha_b e^{i\phi}. \tag{11}$$

The squeezed state in the input mode is divided into two squeezed coherent states in the two output modes. The equation can then be simplified to

$$\begin{aligned}|\psi\rangle_{\rm out} = D(\alpha_b, \sqrt{R'}\hat{A} + \sqrt{T'}\hat{B})\\ S(T\xi_a, \hat{A})S(R\xi_b, \hat{B})|0\rangle_A \otimes |0\rangle_B.\end{aligned} \tag{12}$$

Clearly, the squeezing in both output arms of the beamsplitter will be lower than the one in the input mode. As one can see in equation (12), the two output arms are squeezed coherent states.

The output state in the mode $\hat{A}$ is written as

$$|\psi_{{\rm out},A}\rangle = D(k, \hat{A})S(Tre^{i\omega}, A)|0\rangle_A, \tag{13}$$

where $|k| = \alpha_b\sqrt{R'}$. It is noticeable that the amplitude and squeezing of the output field can be independently adjusted via the amplitude of the input fields, their relative phase, and the beamsplitter reflectance. One can minimize the $g^{(2)}(0)$ function [39] by applying an output state squeezed in the same direction

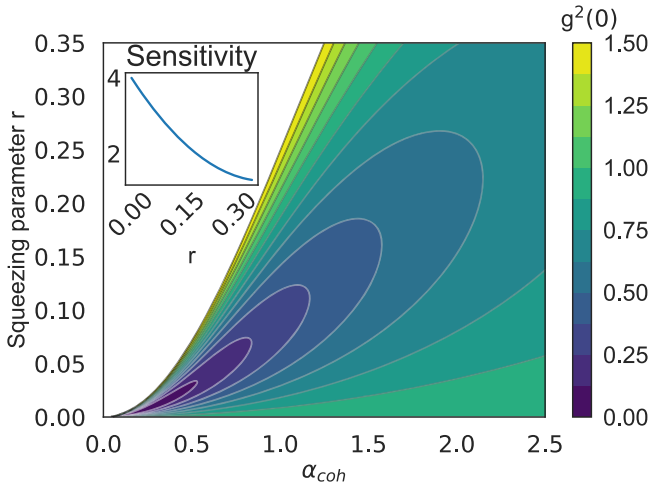

Figure 6. Contour plot of the second-order correlation function in the output mode $\hat{A}$ as a function of the squeezing parameter r of the squeezed vacuum and the amplitude of the coherent state in the input arms, α_{coh}. We consider a beamsplitter with 90% transmission and $\phi = \pi$. It is also important to note that the squeezing direction is aligned with the coherent state. Inset: Sensitivity of the minimum of $g^{(2)}(0)$ ($\partial_r \min_{\alpha_{coh}}[g^{(2)}(0)]$) as a function of the squeezing parameter r.

as the displacement vector (amplitude squeezing), and by choosing the amplitude of the output state as

$$|k| = \sqrt{\frac{\sinh(r/2)\sinh(r)}{e^{-3r/2}(e^{r}-1)}}. \tag{14}$$

If there is only a squeezed vacuum state in one of the input arms ($\alpha_a = 0$) and a coherent state in the other, the highest anti-bunching is found for

$$\phi = \arccos\sqrt{T}/2 - \Phi, \tag{15}$$

$$|\alpha_b| = \frac{1}{\sqrt{R}} e^{r'\sqrt{\frac{R}{T}}} \sqrt{\frac{\sinh(r')\sinh(2r')}{e^{-3r'}(e^{2r'}-1)}}, \tag{16}$$

where $r' = r\sqrt{T}$ and $\alpha_b = |\alpha_b|e^{i\Phi}$. The corresponding correlation function at zero delay $g^{(2)}(0)$ is shown in figure 6, as a function of the squeezing parameter and the amplitude of the input coherent state with a beamsplitter of 90% transmission and a phase difference ϕ fixed to π. In the limit of intense coherent states, this setup is analogous to the homodyne detection and $g^{(2)}(0)$ goes to 1. However, in the limit of weak coherent states, as visible in figure 6, homodyne analogy is not valid anymore, and interestingly, the strongest anti-bunching is obtained for the weakest squeezing. As for the cat state case described previously, there is a limit to the coherent state amplitude that allows for anti-bunching. For large squeezing of the input field, the value of $g^{(2)}(0)$ doesn't go below 1. In analogy to what was shown in the previous section with cat states, mixing an almost vacuum coherent state with an almost weakly squeezed vacuum state leads to the strongest anti-bunching ($g^{(2)}(0) \to 0$). Moreover, as for cat states, one can observe that the correlation function is more sensitive to fluctuations of the squeezing parameter r of the input state for lower squeezing (i.e. small r) (see inset of figure 6). This property can be used to accurately measure weak squeezing. Coincidence measurement as presented here can be advantageously used to characterize weak squeezed states.

Detecting squeezed states and cat states of light is a challenging task. The closer one gets to a coherent state, the higher should be the setup's sensitivity and the more likely one runs into technical difficulties [40, 41]. The present setup actually goes the opposite way, as illustrated in inset of figure 6: getting closer to a coherent state leads to a stronger signature on the $g^{(2)}(0)$ function. This setup can be advantageously employed to witness weakly squeezed or weak cat states. Furthermore, by scanning the amplitude of the input coherent field one can quantify, with a very good accuracy via the $g^{(2)}(0)$ function, how much squeezing is present in the input state or how large the input cat states are. The advantage of this method lies in its simplicity, as it only requires a beamsplitter, a weak coherent beam, and a coincidence measurement setup.

The reason for the observation of anti-bunching behavior by using a cat state or a modified coherent state originates from the fact that the cat states converge to squeezed states for weak amplitudes.

We will now show how this setup is related to the unconventional photon blockade.

3. Unconventional photon blockade

Here, we connect our results to the unconventional photon blockade. This phenomenon typically takes place in a coupled cavity system. Initially, it was studied with both cavities filled with a $\chi^{(3)}$ non-linear medium, resulting in a strong anti-bunched light for a specific set of parameters [12]. Afterwards, it was understood that only one cavity is required to be filled with a non-linear medium to reach the same sub-Poissonian statistics, and that the strong anti-bunching results from destructively interfering optical paths [14, 42]. This mechanism is similar to the one described here.

In order to compare our results from the original proposal with two coupled cavities [12, 14] (c.f. figure 7(b)), we modify the setup proposed by adding a cavity of linewidth γ, filled with a non-linear medium with a non-linearity of 0.01γ, before the beamsplitter (c.f. figure 7(a)). For these parameters, we have numerically estimated the amount of squeezing after the cavity to about 1%. As discussed in section 1, this allows for a very strong anti-bunching after adequate mixing with a coherent state.

In figure 7(c), the correlation function at the output of the setup is plotted in blue as a function of the time delay, normalized to the cavity lifetime. We observe a strong anti-bunching dip, with a linewidth of the same order as the cavity linewidth. For comparison, we plot in red the correlation function one would expect for the same non-linearity in the coupled cavity case. In the same way as for a single-cavity setup, the $g^{(2)}(\tau)$ function vanishes for $\tau \to 0$ but strongly differs for finite delays. While the single-cavity setup leads to a monotonous increase of the $g^{(2)}(\tau)$ to reach 1, the two-cavity setup strongly oscillates at a frequency equal to the cavity linewidth. Moreover,

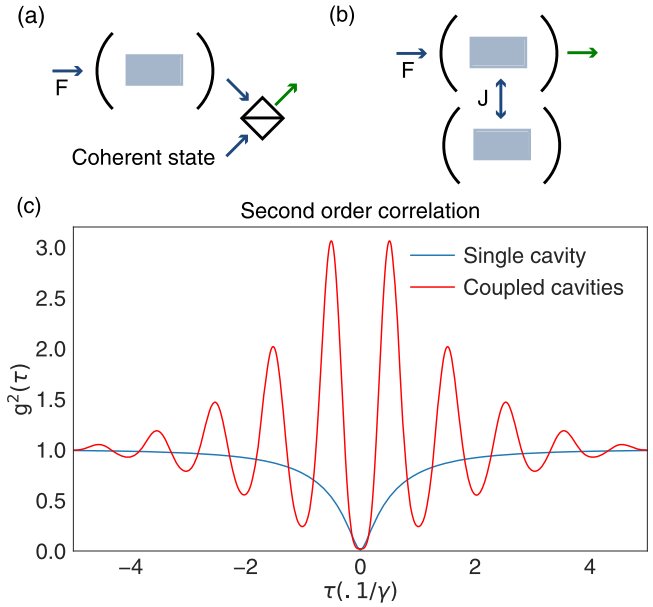

Figure 7. Here, we compare two systems: one consists of a cavity with a non-linear medium of non-linearity $U = 0.01\gamma$, and the other consists of a coupled cavity filled with the same non-linear medium as illustrated in figure 7(a) and 7(b). γ is the cavity linewidth, $J = 6.2\gamma$ is the coupling parameter, F is the feeding rate into the system, and we evaluate $g^{(2)}(\tau)$ in the output path, denoted in green, normalized to the cavity lifetime. All the other parameters are adjusted to have the best anti-bunching in the system.

the amplitude of the oscillation greatly dominates the shot noise value and vanishes for a long time delay.

Strictly speaking, anti-bunching can only be defined for a time window in which $g^{(2)}(\tau)$ increases monotonously with $|\tau|$. Therefore, $g^{(2)}(0) < 1$ is not a sufficient condition [43] for anti-bunching. Consequently, as can be seen in figure 7(c) corresponding to the coupled cavities case (red), one would need to consider only the time window $|\tau| \leqslant \gamma/2$ to actually achieve sub-Poissonian statistics. Hence, in such a configuration, a complex time filtering is necessary to create a strongly anti-bunched state of light. As already pointed out by Flayac and Savona in [42], one can overcome this important limitation and obtain strong anti-bunching with a single cavity by mixing its output with the output of another cavity on a beamsplitter.

The advantage of this setup is that it clearly shows how the two requirements that allow for an unconventional photon blockade, namely weakly nonclassical state and interference, can be met separately. This opens up great possibilities, as it relaxes the constraints on the system parameters to reach the unconventional photon blockade. Generating weakly non-classical states and interfering them with a coherent state are two phenomena that are necessary to obtain strong anti-bunching, but these can be realized and optimized separately.

4. Conclusion

In this article, we focus on a key measurement in quantum optics commonly used to characterize single-photon source: the second-order correlation function, $g^{(2)}(0)$. We show that using a rather simple setup, one can generate strongly anti-bunched states of light ($g^{(2)}(0) \ll 1$). Based on a simple beamsplitter that mixes a coherent field with $g^{(2)}(0) = 1$ with another state characterized by $g^{(2)}(0) > 1$, this setup can provide an output field with $g^{(2)}(0) < 1$. We reveal how this mechanism is a consequence of interfering different Fock state components of the input beams. We consider experimentally feasible conditions and detail how this setup can be advantageously applied to characterize weak squeezed states and Schrödinger cat states. Finally, we connect our results to the unconventional photon blockade to show that both phenomena rely on the same physics. This work offers a simple setup to generate on-demand anti-bunched states of light, which has been found to have many promising applications in the last decade [1]. Moreover, due to its simplicity, the proposed scheme can be easily and efficiently integrated to become a central piece of emerging quantum technologies.

Acknowledgments

The authors would like to thank Cristiano Ciuti and Alejandro Giacomotti for fruitful discussions, and Elisabeth Giacobino for her comments on the manuscript. This work is supported by the French ANR grants (UNIQ DS078, C-FLigHT 138678).

ORCID iDs

Rajiv Boddeda https://orcid.org/0000-0002-4521-0023

References

[1] O'Brien J L, Furusawa A and Vučković J 2009 *Nat. Photonics* **3** 687
[2] Gisin N and Thew R 2007 *Nat. Photonics* **1** 165
[3] Paul H 1982 *Rev. Mod. Phys.* **54** 1061
[4] Schwartz O and Oron D 2012 *Phys. Rev.* A **85** 033812
[5] Schwartz O, Levitt J M, Tenne R, Itzhakov S, Deutsch Z and Oron D 2013 *Nano Lett.* **13** 5832
[6] Michler P, Kiraz A, Becher C, Schoenfeld W, Petroff P, Zhang L, Hu E and Imamoglu A 2000 *Science* **290** 2282
[7] Pisanello F *et al* 2010 *Appl. Phys. Lett.* **96** 033101
[8] Kurtsiefer C, Mayer S, Zarda P and Weinfurter H 2000 *Phys. Rev. Lett.* **85** 290
[9] Aharonovich I, Englund D and Toth M 2016 *Nat. Photonics* **10** 631
[10] Imamog¯lu A, Schmidt H, Woods G and Deutsch M 1997 *Phys. Rev. Lett.* **79** 1467
[11] Birnbaum K M, Boca A, Miller R, Boozer A D, Northup T E and Kimble H J 2005 *Nature* **436** 87
[12] Liew T C H and Savona V 2010 *Phys. Rev. Lett.* **104** 183601
[13] Flayac H and Savona V 2017 *Phys. Rev.* A **96** 053810
[14] Bamba M, Imamoğlu A, Carusotto I and Ciuti C 2011 *Phys. Rev.* A **83** 021802
[15] Snijders H, Frey J, Norman J, Flayac H, Savona V, Gossard A, Bowers J, van Exter M, Bouwmeester D and Löffler W 2018 *Phys. Rev. Lett.* **121** 043601

[16] Vaneph C, Morvan A, Aiello G, Féchant M, Aprili M, Gabelli J and Estève J 2018 *Phys. Rev. Lett.* **121** 043602
[17] Ritze H-H and Bandilla A 1979 *Opt. Commun.* **29** 126
[18] Grankin A, Brion E, Bimbard E, Boddeda R, Usmani I, Ourjoumtsev A and Grangier P 2015 *Phys. Rev. A* **92** 043841
[19] Hong C-K, Ou Z-Y and Mandel L 1987 *Phys. Rev. Lett.* **59** 2044
[20] Grosse N B, Symul T, Stobińska M, Ralph T C and Lam P K 2007 *Phys. Rev. Lett.* **98** 153603
[21] da Silva M P, Bozyigit D, Wallraff A and Blais A 2010 *Phys. Rev.* A **82** 043804
[22] Loudon R 1973 *The Quantum Theory of Light* (Oxford: Clarendon)
[23] Scully M O and Zubairy M S 1997 *Quantum Optics* (Cambridge: Cambridge University Press)
[24] Banerji J 2001 *Pramana* **56** 267
[25] Hickman G T, Pittman T B and Franson J D 2015 *Phys. Rev.* A **92** 053808
[26] Johansson J, Nation P and Nori F 2013 *Comput. Phys. Commun.* **184** 1234
[27] Ourjoumtsev A 2006 *Science* **312** 83
[28] Ourjoumtsev A, Jeong H, Tualle-Brouri R and Grangier P 2007 *Nature* **448** 784
[29] Stobińska M, Milburn G J and Wódkiewicz K 2007 *Open Syst. Inf. Dynamics* **14** 81
[30] Huang K *et al* 2015 *Phys. Rev. Lett.* **115** 023602
[31] Wu L-A, Kimble H J, Hall J L and Wu H 1986 *Phys. Rev. Lett.* **57** 2520
[32] Bergman K and Haus H A 1991 *Opt. Lett.* **16** 663
[33] Machida S, Yamamoto Y and Itaya Y 1987 *Phys. Rev. Lett.* **58** 1000
[34] Glorieux Q, Dubessy R, Guibal S, Guidoni L, Likforman J-P, Coudreau T and Arimondo E 2010 *Phys. Rev.* A **82** 033819
[35] Glorieux Q, Guidoni L, Guibal S, Likforman J-P and Coudreau T 2011 *Phys. Rev.* A **84** 053826
[36] Corzo N V, Glorieux Q, Marino A M, Clark J B, Glasser R T and Lett P D 2013 *Phys. Rev.* A **88** 043836
[37] Gong J J and Aravind P K 1990 *Am. J. Phys.* **58** 1003
[38] Lvovsky A I 2015 *Photonics* (New York: Wiley) pp 121–63
[39] Lemonde M-A, Didier N and Clerk A A 2014 *Phys. Rev.* A **90** 063824
[40] Ourjoumtsev A, Kubanek A, Koch M, Sames C, Pinkse P W H, Rempe G and Murr K 2011 *Nature* **474** 623
[41] Glorieux Q, Clark J B, Corzo N V and Lett P D 2012 *New J. Phys.* **14** 123024
[42] Flayac H and Savona V 2017 *Phys. Rev.* A **96** 053810
[43] Zou X T and Mandel L 1990 *Phys. Rev.* A **41** 475